Determining the Structure of Trimethylphosphine Bound to the Brønsted Acid Site in Zeolite HY: Double-Resonance NMR and ab Initio Studies

Hsien-Ming Kao,[†,‡] Haiming Liu,[†] Jyh-Chiang Jiang,[§] Sheng-Hsien Lin,[§] and Clare P. Grey*[,†]

Department of Chemistry, State University of New York at Stony Brook, Stony Brook, New York 11794-3400, and Institute of Atomic and Molecular Sciences, Academic Sinica, Taipei, Taiwan, Republic of China

Received: November 30, 1999; In Final Form: March 7, 2000

Solid-state NMR methods and ab initio calculations have been employed to investigate the structure of the trimethylphosphine (TMP)−Brønsted acid site complex in zeolite HY. $^{27}Al/^{31}P$ and $^{27}Al/^{1}H$ rotational echo double-resonance NMR experiments performed at −150 °C were utilized to measure Al−P and Al−H_B distances for the acid site−TMP complex of 3.95 (±0.05) and 2.8−3.1 Å, respectively, where H_B is the Brønsted acid site proton. A more accurate measurement of the Al−H_B distance was not possible since models that assume the presence of isolated Al−H spin pairs are not valid in this case. A P−H_B distance of 1.40 (±0.02) Å was obtained by fitting the spinning sidebands in the ^{1}H magic angle spinning (MAS) NMR spectrum. These internuclear distances are within the range of the Al−P, Al−H_B, and P−H_B distances obtained from ab initio calculations for the ion pair (IP) $TMPH^+$−zeolite complex that is formed by transferring a Brønsted acid proton to TMP. In contrast to the ^{31}P MAS NMR spectra, which indicated that the only stable species was $TMPH^+$, ab initio calculations on small cluster models predicted that the neutral complex should be more stable than the IP complex. However, use of a larger zeolite fragment in the calculations enhanced the relative stability of the IP structure.

I. Introduction

An understanding of acid strength, and the role of the framework in controlling this, is fundamental to the understanding of acid-catalyzed reactions in zeolites. Sorption of basic molecules on acidic catalysts, in combination with temperature-programmed desorption or calorimetry, is one method used to characterize the solid acidity. Infrared (IR) and magic angle spinning (MAS) NMR spectroscopies are also widely used to investigate the interactions between these probe molecules and the Brønsted acid sites. Research in this area has been extensively reviewed in refs 1 and 2. More recently, quantum mechanical methods have also been used to determine the energetics of proton transfer from the zeolite framework to the adsorbed molecules and the structures of the acid−base complexes.[3,4] Particular attention has been paid to the question of whether protonated (ionic) surface species arise as transition states in the reaction path or whether they exist as distinct intermediates.[3] In the latter case, these ionic species will be present in equilibrium with "neutral" hydrogen-bonded complexes, i.e.

$$B\cdots HZ \leftrightarrow BH^+\cdots Z^-$$

where B is an adsorbed basic molecule and HZ represents a protonated zeolite. In some systems, particularly those involving weak bases, much conflicting experimental and theoretical data exists. For example, the exact nature of the surface species on sorption of water, methanol, or acetonitrile on zeolitic Brønsted acid sites still remains a matter of discussion.[5−8]

One of the aims of the study presented in this paper is to explore the feasibility of using double-resonance methods designed for measuring internuclear distances to determine the mode of binding of probe molecules to the Brønsted acid site in zeolites. Although MAS NMR has been extensively used to study gas sorption of basic probe molecules, only a few studies have exploited NMR methods that allow connectivities, or distances between spins on the site of adsorption and on the adsorbed molecule, to be determined.[9−11] In earlier work, we used $^{15}N-^{27}Al$ rotational echo double-resonance (REDOR) NMR to measure the distance between the aluminum T-sites in zeolite HY and the nitrogen atom in ^{15}N-enriched monomethylamine (MMA).[9] Our $^{15}N-^{27}Al$ distance of 3.1 Å was consistent with models for $MMAH^+$ binding involving two or three hydrogen bonds as predicted by the calculations of Teunissen and van Santen for NH_3 binding on acidic zeolitic clusters.[12] In this paper, we describe a more detailed study of the binding of trimethylphosphine on the zeolite HY. A goal of these experiments is to compare the NMR results with those from ab initio calculations involving small model clusters and to explore the limits and applicability of the NMR double-resonance methods. In particular, we explain some of the approaches that we have adopted to help overcome some of the difficulties encountered in studying this and other systems.

We have chosen the probe molecule trimethylphosphine (TMP), in view of the previous NMR studies using this molecule on zeolites[13−15] and, e.g., sulfated zirconias[16] and the sensitivity (large γ and 100% natural abundance) of the ^{31}P nucleus. The field has been reviewed in ref 17. Unlike MMA, which we used in our previous REDOR study, TMP does not require any isotopic labeling. In addition, binding of this molecule is expected to be less complicated than that of some other widely

* Corresponding author. Phone: (631) 632-9548. Fax: (631) 632-5731. E-mail: cgrey@sbchem.sunysb.edu.
† State University of New York at Stony Brook.
‡ Current address: Department of Chemistry, National Central University, Chung-Li, Taiwan 32054.
§ Academic Sinica.

10.1021/jp994199h CCC: $19.00
Published on Web 04/26/2000

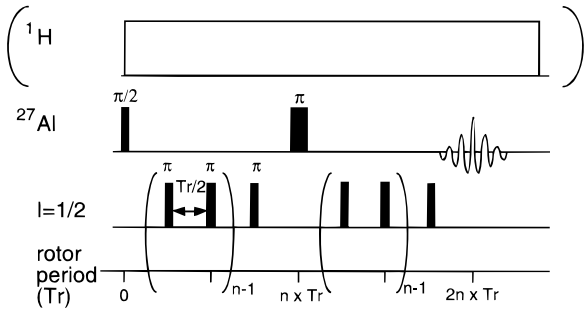

Figure 1. Pulse sequences used in the ^{27}Al/^{31}P and ^{27}Al/^{1}H REDOR NMR experiments. A string of π pulses was applied to the $I = 1/2$ (^{31}P or ^{1}H) nuclei. These pulses are omitted in the control experiment. ^{1}H decoupling was applied in the ^{27}Al/^{31}P REDOR sequence only.

studied basic molecules such as water, methanol, and many amines, since extensive hydrogen-bonding networks are not formed.

NMR methods for measuring internuclear distances are based on the determination of the dipolar coupling between two spins. In the absence of any motion, this dipolar coupling is inversely proportional to the cube of the distance between the spins. However, the dipolar coupling, even between nearby spins, is often very small on the time scale of many motional processes (e.g., a ^{27}Al$-^{15}$N distance of 3.1 Å corresponds to a dipolar coupling of 0.1 kHz). Thus, any residual motion at or faster than this time scale (generally more than $1-10$ ms) will reduce or, for isotropic motion, average the measured dipolar coupling constant to zero, resulting in a longer than expected distance. This typically requires that any experiments involving molecules sorbed on surfaces be performed at low temperatures, where the translational motion of the molecules will be frozen out. Any remaining motion (e.g., librations) of the molecule on the surface will similarly reduce the measured dipolar coupling, and in some circumstances, it may be appropriate to consider the NMR experiment as a method for determining the maximum internuclear distance between spins. For the TMP$-$zeolite system, Lunsford demonstrated that the motion of TMPH$^+$ complexes in zeolites such as HY, dealuminated HY, and HZSM-5 was strongly affected by the size of the cavities and/or channels, and the temperature of the sample.[18] The motion of TMP has also been studied as a function of temperature by Bendada et al.,[15] and ourselves.[19,20] Exchange between different binding sites was shown to be frozen out at low temperatures.[19,20] Fyfe and Lewis have also discussed the need to consider mobility of the probe molecules when measuring internuclear distances between the sorbent and substrate.[21]

Two standard methods for measuring the dipolar coupling under MAS conditions were employed. Small dipolar coupling constants were determined with REDOR NMR,[23,23] while much larger dipolar coupling constants were obtained directly from a one-pulse experiment, by fitting the spinning sideband intensities. In one variant of the REDOR method,[23] π pulses are applied to one of the coupled nuclei, while an echo sequence is applied to the other nucleus (see Figure 1). Thus, one requirement of the REDOR experiment for distance measurement is that the π pulses affect both spins in a predictable fashion (i.e., the response to a π pulse can be readily calculated). This requirement is not always readily satisfied when one set of nuclei is quadrupolar (e.g., ^{27}Al; $I = 5/2$). For this reason, the spin$-$echo sequence was applied to the quadrupolar nucleus, and thus, only the effect of the π pulses applied to the $S = 1/2$ spins (^{31}P/^{1}H) on the $I = 5/2$ central transition (transverse) coherence ($|+1/2\rangle \pm |-1/2\rangle$) needs to be calculated. Other variations of the REDOR method[19] were not used, since they require the application of a string of π pulses to the ^{27}Al spins.

One problem we have also needed to address for many catalyst systems containing aluminum atoms is the "invisible" nature of many aluminum surface sites, as probed by MAS NMR. The ^{27}Al central transition is broadened by the second-order quadrupolar interaction, which may sometimes be so large as to render the ^{27}Al spins invisible when standard one-pulse methods are used. This is the case for the aluminum atoms in the Brønsted acid site in dehydrated zeolites.[24,25] In our previous ^{27}Al/^{15}N REDOR study of MMA on zeolite HY, we exploited the fact that the quadrupole coupling constants (QCCs) of the aluminum site, and hence the second-order quadrupolar interaction, is reduced by the sorption of the basic probe molecule: one aluminum atom becomes "visible" per adsorbed probe molecule.[9] Thus, in these types of systems, the fraction of visible aluminum should be accurately determined, in order to analyze the REDOR data.

The other approach we have taken is to detect the invisible spins indirectly via their dipolar coupling to other nearby nuclei through the use of the TRAPDOR (Transfer of Populations in Double-Resonance) NMR method. We have previously used this experiment to determine the ^{27}Al quadrupole coupling constants of different invisible aluminum environments in steamed and unsteamed zeolites, and to characterize the aluminum Lewis and Brønsted acid sites.[19,24,26] ^{27}Al/^{31}P TRAPDOR methods have also been used to demonstrate the binding of the probe molecules trimethylphosphine oxide to the Lewis sites in USY.[27] Because the TRAPDOR data are dependent on a large number of variables, in addition to the dipolar coupling, this method does not yield accurate distance information. However, our recent studies indicate that if the quadrupole coupling constants are determined by measuring the TRAPDOR fractions as a function of the ^{27}Al offset frequency, then accurate simulations of the TRAPDOR dephasing curves (and thus an estimate of the internuclear distance) may sometimes be possible.[28]

II. Experimental Section

Sample Preparation. The protonated form of zeolite Y (HY) was prepared by deammoniation of NH_4Y (Linde, LZY-62, Si/Al = 2.6). A two-step calcination procedure, similar to that used by Luz and Vega,[29] was used to prepare the samples. First, a sample was dehydrated under vacuum by slowly ramping the temperature to 110 °C over a period of 7 h (or more). The sample was then deammoniated by ramping the temperature, over at least 12 h, to 400 °C; the sample was kept at this temperature for another 12 h until the pressure dropped to below 10^{-3} Torr. The resulting material was characterized by ^{1}H MAS NMR. TMP (Alfa, 99%) was introduced into the samples at room temperature over the vacuum line, and samples with different loading levels were prepared by monitoring the drop in pressure. Typically, samples with loading levels in the range of $16-24$ TMP per unit cell (uc) were used in the REDOR NMR experiments. The samples were denoted as *x*TMP/HY, where *x* represents the loading level of TMP per unit cell.

NMR Experiments. NMR experiments were performed on a Chemagnetics CMX-360 spectrometer, equipped with a Chemagnetics triply tuned 7.5 or 5.0 mm probe, with resonance frequencies for ^{27}Al and ^{31}P of 93.82 and 145.74 MHz, respectively. The $\pi/2$ pulse lengths for ^{1}H, ^{31}P, and ^{27}Al were typically 4.0, 6.5, and 4.5 μs, respectively. The ^{27}Al and ^{31}P chemical shifts were externally referenced to a saturated aqueous aluminum sulfate solution and 85% H_3PO_4, respectively.

Detailed experimental conditions used to acquire the various spectra are given below and in the figure captions.

$^1H \rightarrow {}^{31}P$ and $^{31}P \rightarrow {}^1H$ Cross Polarization (CP). The Hartmann−Hahn condition for $^1H \leftrightarrow {}^{31}P$ CP experiments was determined using $(NH_4)_2HPO_4$. The optimal contact time for CP was found to be 1 ms. Repetition times of 2 and 5 s were used in the $^1H \rightarrow {}^{31}P$ and $^{31}P \rightarrow {}^1H$ CP experiments, respectively.

^{27}Al and ^{31}P Spin Counting. ^{27}Al and ^{31}P spin counting was performed by comparing the integrated intensities of zeolite samples of known mass with those of aluminum acetylacetonate and $(NH_4)_2HPO_4$, respectively. The ^{27}Al nutation frequency of the central (i.e., $|1/2\rangle \leftrightarrow |-1/2\rangle$) transition will vary according to the size of the QCCs of the aluminum sites. Thus, ^{27}Al MAS NMR spectra were obtained with small flip angles of approximately 15° to make a quantitative comparison of the numbers of ^{27}Al spins.[30] Only the ^{27}Al central transition was visible for the zeolite samples in the ^{27}Al spectrum. For aluminum acetylacetonate, however, the outer satellite transitions were visible. Thus, the graphical method of Massiot et al.[31] was used to determine the contribution of the outer satellite transitions to the intensity of the isotropic resonance of aluminum acetylacetonate, and the percentage of the central transition intensity, present in the spinning sidebands. Both these contributions were found to be negligible (<1%) for the spinning speeds typically used (8−10 kHz). Thus, the intensity of the central transition of aluminum acetylacetonate could be directly compared with the intensities observed for the zeolite samples. No noticeable changes in the Q of the probe between the different zeolite samples and the spin-counting standards were observed; thus, no additional corrections were performed. Repetition times of 3 and 60 s were used to collect the ^{27}Al and ^{31}P MAS spectra, respectively.

REDOR NMR. The pulse sequences used for the $^{27}Al/^{31}P$ and $^{27}Al/^1H$ REDOR experiments are shown in Figure 1. XY-8 compensated phase cycling[23] was used on the ^{31}P or ^1H channels to minimize off-resonance effects and the effect of rf field power fluctuations during the REDOR measurements. The ^{27}Al spins were monitored, and thus short pulses (e.g., 1 and 2 μs for the $\pi/2$ and π pulses, respectively) were applied to the ^{27}Al spins, to ensure that the whole solid sample was uniformly excited. The intensities of the ^{27}Al echoes, measured with and without applying a series of π pulses (either ^{31}P or ^1H) at half-integral multiples of the rotor cycles, are denoted as S_f and S_0, respectively. If n is the total number of dephasing rotor periods and $T_r = 2\pi/\omega_r$ is the rotor period, where ω_r is the spinning speed, then for an isolated pair of nuclei the dipolar dephasing of the REDOR signal is[22]

$$\Delta\Phi_n = n4\sqrt{2}DT_r \sin\alpha \sin\beta \cos\beta \qquad (1)$$

where $D = \gamma_I\gamma_S\hbar/2\pi r^3$ is the strength of the dipolar coupling, γ_I and γ_S are the magnetogyric ratios of the I and S spins, respectively, $\hbar$ is Planck's constant, r is the internuclear distance between I and S, and the angles α and β describe the orientation of the internuclear vector in the MAS reference frame. The expected difference signal, normalized to the full echo intensity, i.e., the REDOR fraction, is calculated by an average over all possible internuclear vector orientations:[22]

$$(\Delta S/S_0)_n = 1 - (1/4\pi)\int_0^{2\pi} d\alpha \int_0^{\pi} \sin\beta\, d\beta \cos(\Delta\Phi_n) \qquad (2)$$

where ΔS is the difference in intensity between S_0 and S_f. Experimentally, π pulse lengths were adjusted slightly for the solid sample to obtain the maximum degree of the REDOR dephasing for a fixed number of rotor cycles.

The finite length of the ^1H or ^{31}P π pulse will not significantly affect the REDOR dephasing provided that the combined time periods of all the different ^1H or ^{31}P pulses correspond to less than 10% of the rotor period.[32] Since two ^{31}P π pulses of time interval 10−12 μs were used (and the ^1H pulse lengths are even shorter) per rotor period, for a spinning speed of 2 kHz, the effect of finite lengths of π pulses on the REDOR dephasing is negligible under the conditions typically used in this paper and was not considered in the analysis of the REDOR data.

TRAPDOR NMR. The pulse sequences used in the $^{31}P/^{27}Al$ and $^1H/^{27}Al$ TRAPDOR NMR experiments are similar to those used in refs 19 and 24, respectively. The ^{31}P magnetization was prepared via $^1H \rightarrow {}^{31}P$ CP in the $^{31}P/^{27}Al$ TRAPDOR experiments, while $^{31}P \rightarrow {}^1H$ CP was used in the $^1H/^{27}Al$ TRAPDOR experiments. A comprehensive description of the method with experimental details has been given in our earlier publications.[20,24] Experiments were performed with and without ^{27}Al irradiation during the evolution period, τ, of the $I = 1/2$ rotor-synchronized spin−echo experiment, the latter experiment serving as a control to eliminate spin−spin relaxation (T_2) effects. The ^{27}Al irradiation time period was incremented by increasing the number of rotor periods of ^{27}Al irradiation, and S_f and S_0 were measured for each time increment, where S_f and S_0 are the echo intensities measured with and without ^{27}Al irradiation. All TRAPDOR NMR experiments were performed at close to on-resonance irradiation conditions, with an ^{27}Al rf field amplitude of 58 kHz.

Calculations of the experimentally determined $^{27}Al/^{31}P$ TRAPDOR fraction ($1 - S_f/S_0$ ($=\Delta S/S_0$); cf. the REDOR fraction) were performed numerically. The program used in these simulations calculates the time evolution of the propagator of the time-dependent (quadrupolar and dipolar) Hamiltonian for small time intervals during the ^{27}Al rotor period.[33]

Models and Calculation Methods. All the calculations have been performed with the GAUSSIAN92 program[34] using the 6-31G* basis set at the Hartree−Fock self-consistent field (HF-SCF) level.[35] Where required, electron correlation effects for valence electrons were corrected up to second order in the energy by using Møller−Plesset perturbation theory (MP2).[36] The geometries were fully optimized by means of analytical gradients. The interaction energies of complexes were corrected for the basis set superposition error (BSSE) with a standard Boys−Bernardi counterpoise correction scheme[37] and zero-point vibrational energy (ZPVE). Two zeolite cluster models were used in this work, $H_3Si-OH-AlH_3$ (Z_1H) and $H_3Si-OH-Al(OSiH_3)_3$ (Z_2H). To preserve the correct charge and spin multiplicity of the model, the "dangling" bonds that would connect the model with the rest of the solid were saturated with hydrogen atoms.[12] In the case of Z_1H, the active site was represented by a tetrahedral aluminum atom linked by an OH group to a silicon atom. The second model, Z_2H, represents a complete second coordination sphere of four silicon atoms around a central Al atom. Such a model allowed us to investigate binding to the acidic OH bridge and its neighboring basic oxygen atoms on the adjacent Si−O−Al bridges, simultaneously. The geometries were fully optimized at both HF/6-31G* and MP2/6-31G* levels for the Z_1H cluster. The geometries were optimized at the HF/6-31G* level for Z_2H, and fully optimized and single-point MP2 energies were then calculated with these HF/6-31G* geometries.

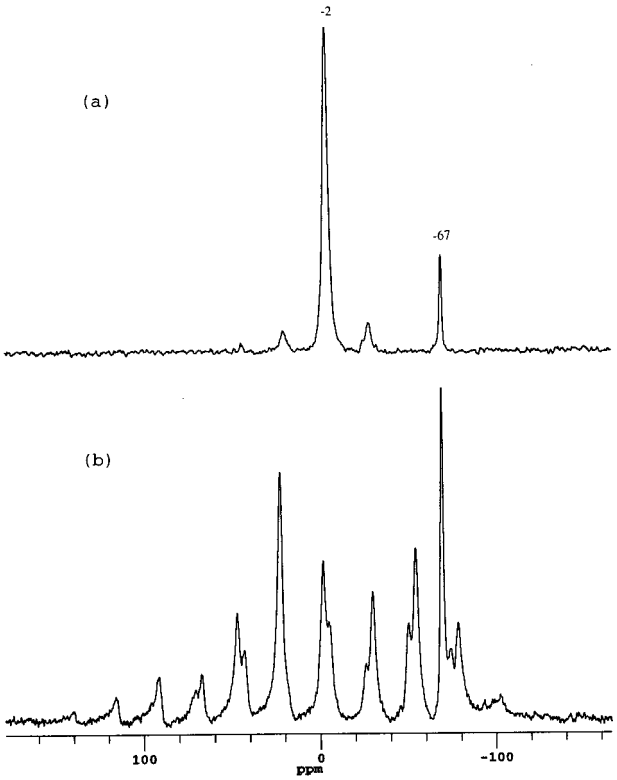

Figure 2. $^{1}H \rightarrow {}^{31}P$ CP spectra of 30TMP/HY obtained at room temperature (a) with and (b) without ^{1}H decoupling at a spinning speed of 3500 Hz. The isotropic resonances are labeled in (a), and other peaks in this spectrum are spinning sidebands. (Contact time = 1 ms.)

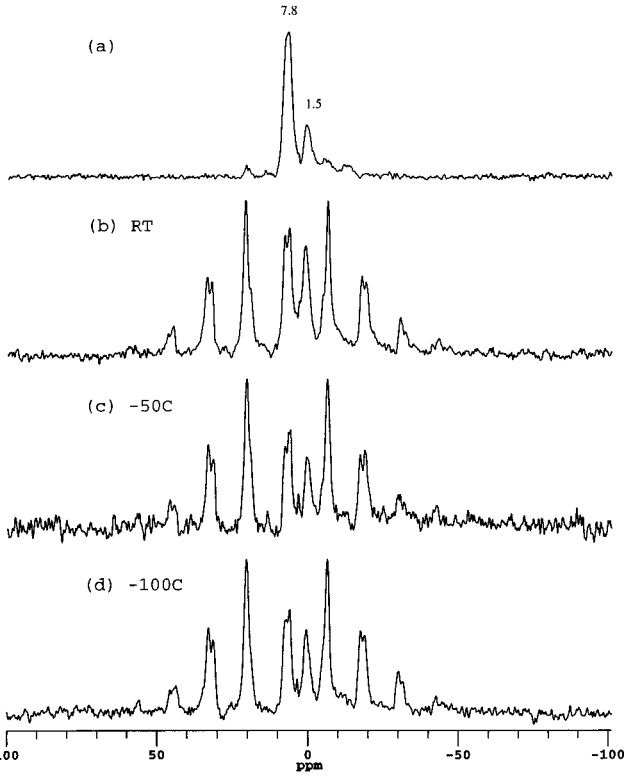

Figure 3. $^{31}P \rightarrow {}^{1}H$ CP spectra of 19TMP/HY obtained (a) at room temperature with ^{31}P decoupling and (b−d) without ^{31}P decoupling at room temperature and −50 and −100 °C, respectively, at a spinning speed of 4470 Hz. (Contact time = 1 ms. The isotropic resonances are labeled in (a), and other peaks in this spectrum are spinning sidebands.)

III. Results

HY. The ^{1}H MAS NMR spectrum (not shown) of dehydrated zeolite HY consists, in agreement with previous NMR studies of HY zeolites, of a resonance at 3.6 ppm and a shoulder around 4.6 ppm, which can be assigned to the protons pointing into supercages and sodalite cages, respectively.[37] The intensity of the resonance due to ammonium cations, at around 7 ppm, was negligible, confirming the nearly complete deammoniation of NH_4Y.

$^{1}H \rightarrow {}^{31}P$ and $^{31}P \rightarrow {}^{1}H$ Cross Polarization. Conventional $^{1}H \rightarrow {}^{31}P$ CP MAS NMR spectra of 30TMP/HY (i.e., a sample with 30 TMP molecules per unit cell), with and without proton high-power decoupling, are shown in parts a and b, respectively, of Figure 2. The ^{31}P resonance at −2 ppm is due to $TMPH^+$. As in the previous study of Lunsford et al.[13,14] a $^{31}P-{}^{1}H$ J coupling constant of approximately 550 Hz (Figure 2b) and large spinning sideband manifolds are observed. The intensities of the sideband manifolds for $TMPH^+$ in LaY have been analyzed to obtain a P−H distance of 1.42 Å in their system.[14] The resonance at −67 ppm is assigned to liquidlike TMP species and only appears at high loading levels (more than approximately 24 TMP/uc). Variable-temperature $^{31}P \rightarrow {}^{1}H$ CP MAS spectra of 19 TMP/uc, with and without ^{31}P decoupling, are shown in Figure 3. The $^{31}P \rightarrow {}^{1}H$ CP experiments were performed to enhance the intensity of the "$P-H^+$" resonance, in comparison to that of the CH_3 groups. The ^{1}H resonances at 7.5 and 1.1 ppm (seen most clearly in the spectrum acquired with ^{31}P decoupling, Figure 3a) are assigned to protons directly attached to the phosphorus atoms and the three methyl groups of $TMPH^+$, respectively. In the absence of ^{31}P decoupling during the acquisition period, the resonance at 7.5 ppm splits into a doublet, due to $^{31}P-{}^{1}H$ J coupling, and a sideband envelope that resembles a Pake doublet is observed, resulting from the large P−H dipolar coupling (∼18 kHz). Upon cooling to −50 °C, a reduction of the intensity of the center peak of the sideband pattern is seen, consistent with a decrease in the mobility of $TMPH^+$ (Figure 3c). No further spectral changes are observed at lower temperatures (e.g., at −100 °C) (Figure 3d), indicating that $TMPH^+$ is rigid on the time scale of the P−H dipolar coupling. A simulation of the $TMPH^+$ spectrum at −100 °C is shown in Figure 4. Unlike Chu et al.,[14] we have chosen to simulate the ^{1}H spectra as opposed to the ^{31}P spectrum since the ^{1}H CSA is much smaller (see Figure 3a) than the ^{31}P CSA and, to a first approximation, may be ignored. A good fit could be obtained with a $^{1}H-{}^{31}P$ dipolar coupling constant of 17.5 kHz, but the fit could be slightly improved if a small ^{1}H CSA with an anisotropy of 2.8 ppm (and an asymmetry parameter of 0) was included in the simulation (Figure 4). A dipolar coupling constant of 17.5 kHz corresponds to a P−H distance

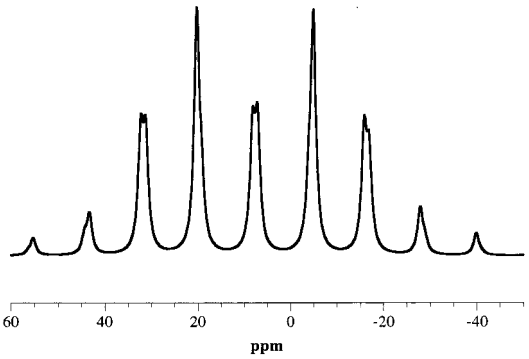

Figure 4. Simulation of the ^{1}H MAS NMR spectra of 19TMP/HY. $^{31}P/^{1}H$ dipolar coupling constant = 17.5 kHz. CSA parameters: anisotropy = 2.8 ppm (i.e., 1.0 kHz), $\eta = 0$. The CSA and dipolar tensors were assumed to be collinear; spinning speed = 4470 Hz.

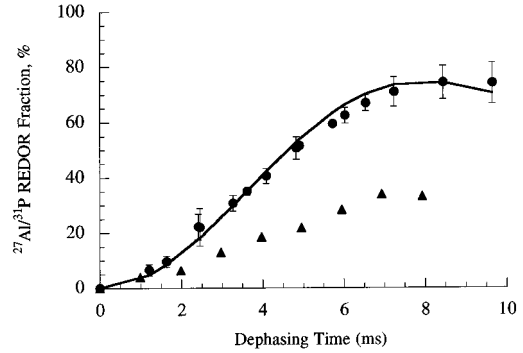

Figure 5. ^{27}Al/^{31}P REDOR dephasing for 18TMP/HY-a. Data were collected at room temperature (triangles) and −150 °C (circles). The former was acquired at a spinning speed of 2020 Hz, and the latter at spinning speeds of 1660 and 2045 Hz. The simulated curve (solid line) was calculated with a dilution factor of 0.72 and a dipolar coupling constant of 210 Hz.

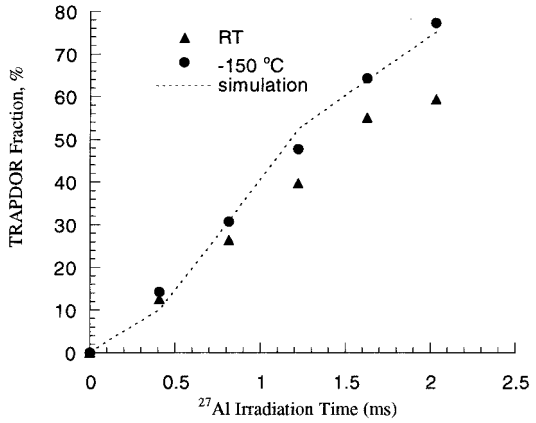

Figure 6. ^{31}P/^{27}Al TRAPDOR fraction as a function of ^{27}Al irradiation time (for close to on-resonance irradiation) obtained for 21TMP/HY at room temperature (traingles) and −150 °C (circles). Spinning speed = 2.46 kHz, and ^{27}Al rf field strength = 58 kHz; the dashed line shows the simulated dephasing curve (see the text).

of 1.40 Å. The dipolar coupling and CSA tensors were assumed to be collinear (which was observed previously for the ^{31}P CSA and the dipolar coupling tensor), which produced the best fit to the experimental data. The CSA is so small, however, that small variations in the relative orientation of the two tensors do not change the quality of the fit significantly. Nonetheless, even if we assume that the orientation of the two tensors represents the major source of error in the distance measurements, this only introduces an error of ±0.015 Å to the determination of the P−H distance. Changes in the dipolar coupling constant of ±1000 Hz introduce noticeable changes in the ratios of the spinning sidebands, and a poorer fit. Thus, we estimate that our distance measurements are accurate to within ±0.025 Å. The measured P−H distance of 1.40 (±0.025 Å) is close to the distance of 1.420 Å found for typical P−H bonds in phosphines.[39] We did not perform any further analyses of these spectra as the P−H dipolar coupling has been previously studied in much greater detail for analogous systems.[14]

^{27}Al MAS NMR. ^{27}Al MAS NMR spectra of HY loaded with TMP all show a resonance at approximately 57 ppm, from the four-coordinated, or T-site, aluminum atoms of the zeolite framework. No resonances due to extraframework, octahedral aluminum atoms were observed.

^{27}Al and ^{31}P Spin Counting. Spin-counting results, for all the samples with loading levels of 16−24 TMP molecules per unit cell, showed P:Al ratios that varied between 0.6:1 and 0.8:1. In particular, P:Al ratios of 0.72 and 0.65 were determined for the two different samples with the same loading level, 18TMP/HY-a and 18TMP/HY-b, which were used in the ^{27}Al/^{31}P and ^{27}Al/^{1}H REDOR NMR experiments described below, respectively. Thus, 25 and 27.7 aluminum atoms are visible per unit cell, for 18 sorbed TMP molecules, for the two samples, respectively. The intensity of ^{31}P signal did not change when a longer repetition time of 120 s was employed. Thus, we can conclude that some of the visible ^{27}Al spins are not directly bound to a TMP complex.

^{27}Al/^{31}P REDOR NMR. ^{27}Al/^{31}P REDOR NMR experiments were performed at room temperature and −50, −100, and −150 °C; the reduction in the intensity of the ^{27}Al echo ($\Delta S/S_0$) (or REDOR fraction) extracted from spectra collected at room temperature and −150 °C is shown in Figure 5. Upon cooling the sample from room temperature to −50 °C, a significant loss in ^{27}Al intensity in the REDOR experiment (and thus a larger REDOR fraction) was observed. Similar REDOR fractions were, however, observed, for the same dephasing time, at −50, −100, and −150 °C. This indicates that any significant $TMPH^+$ motion is frozen out by −50 °C; no further residual motion (if there is any) is frozen out, on the REDOR time scale from −50 to −150 °C. From the ^{27}Al and ^{31}P spin-counting results, only 72% of the observable ^{27}Al spins are bound or coupled to the ^{31}P spins of $TMPH^+$, in this particular sample. This calculation assumes that a 1:1 complex for TMP bound to the Brønsted acid site is formed, a reasonable assumption at this relatively low TMP loading level. Thus, the REDOR dephasing curves were fit by using a modified version of eq 2, in which the REDOR fractions ($\Delta S/S_0$) were multiplied by a dilution factor of 0.72, to take into account the number of dipolar coupled spins. The best fit to the REDOR data collected at −150 °C was obtained with a dipolar coupling constant of 210 Hz (solid line in Figure 5) which, assuming no motional averaging, corresponds to an Al−P distance of 3.95 (±0.05) Å. Note that the maximum reached in our REDOR dephasing curve just after it starts to flatten out (75 ± 5%) is close to that predicted from our spin-counting results (72%), in agreement with the 1:1 assumption for complex formation.

^{27}Al/^{31}P TRAPDOR NMR. ^{27}Al/^{31}P TRAPDOR NMR experiments were performed at −150 °C, and a plot of the TRAPDOR fraction as a function of the ^{27}Al irradiation time is shown in Figure 6. The TRAPDOR fraction increased with ^{27}Al irradiation time, indicating that the $TMPH^+$ molecule is in close proximity to an aluminum atom. Similar TRAPDOR fractions were observed at −100 °C, in comparison to those obtained at −150 °C, but reduced fractions were seen at room temperature (triangles, Figure 6), again suggesting that the $TMPH^+$ molecules are rigid below −100 °C, on the time scale of the ^{27}Al/^{31}P coupling; this is consistent with the ^{27}Al/^{31}P REDOR NMR shown above. The ^{27}Al/^{31}P TRAPDOR fractions increase much more rapidly at all temperatures, as a function of the dephasing time, than the REDOR fractions, which is consistent with the larger dipolar couplings measured by the TRAPDOR experiment, since coupling to all the ^{27}Al Zeeman levels (and not just the two central levels, $|\pm 1/2\rangle$) are measured in this experiment.

^{27}Al/^{1}H REDOR NMR. Figure 7a shows the dephasing curves in the ^{27}Al/^{1}H REDOR experiments, collected at room temperature and at −150 °C. Again, the REDOR fractions were smaller at room temperature. The ^{27}Al and ^{31}P spin-counting experiments for the material studied by ^{27}Al/^{1}H REDOR NMR indicated that only 65% of the visible aluminum atoms are bound to a TMP molecule, assuming the formation of a 1:1 complex for TMP bound to the Brønsted acid site. The fit to the REDOR data shown in Figure 6a was obtained by assuming

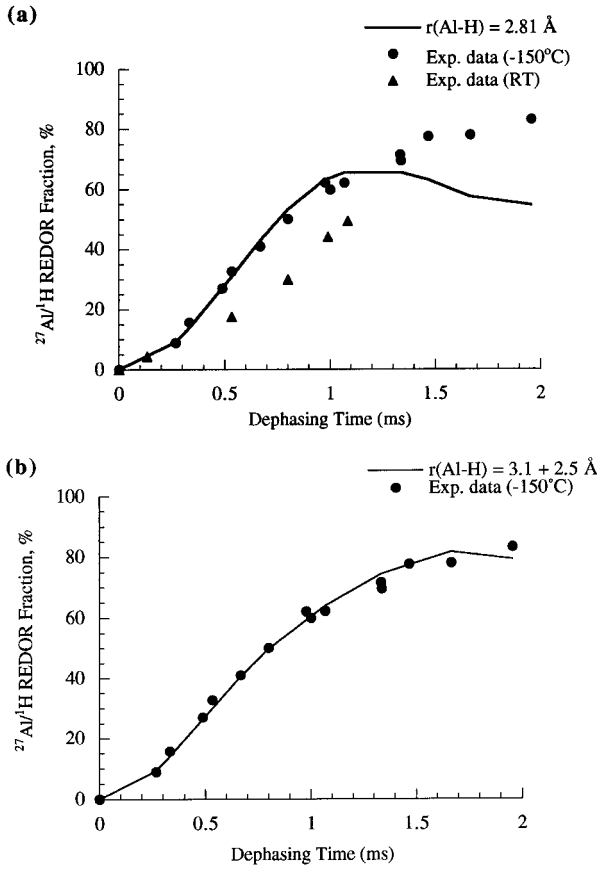

Figure 7. (a) ^{27}Al/^{1}H REDOR fraction for 18TMP/HY-b as a function of the dephasing time obtained at room temperature (triangles) and −150 °C (circles). The simulated curve (solid line) was calculated with a dilution factor of 0.65 and a ^{27}Al/^{1}H dipolar coupling constant of 1400 Hz (corresponding to an Al−H_B distance of 2.81 Å). (b) The best fit to the low-temperature data when 15% of the visible ^{27}Al spins are assumed to result from Brønsted acid sites (Al−H_B = 2.45 Å). The curve is a sum of two REDOR curves, one with a dilution factor of 0.65 and a ^{27}Al/^{1}H dipolar coupling constant of 1000 Hz (Al−H_B distance = 3.10 Å), and the other with a dilution factor of 0.15 and a dipolar coupling constant of 2120 Hz (2.45 Å) (see the text).

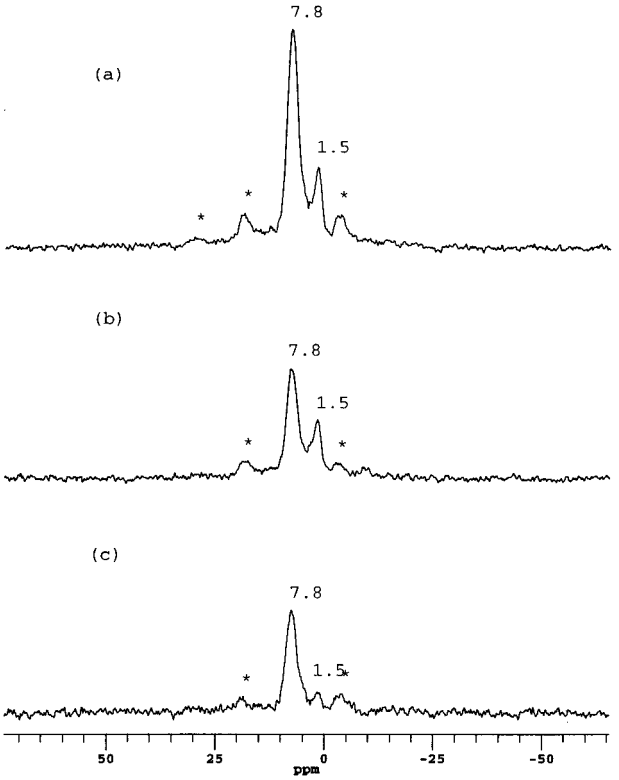

Figure 8. ^{1}H/^{27}Al TRAPDOR spectra of 18TMP/HY-b. ^{1}H magnetization was prepared via a ^{31}P → ^{1}H CP experiment, to select the protons near TMP. (a) No ^{27}Al irradiation (the control experiment). (b) ^{27}Al irradiation. (c) Difference spectrum (a) − (b). (Contact time = 1 ms, spinning speed = 4 kHz, and ^{27}Al irradiation time = 1 ms, i.e., 4 rotor periods.)

that the remaining 35% of the aluminum spins are far from any ^{1}H spins and do not contribute to the dephasing. This curve corresponds to a ^{27}Al/^{1}H dipolar coupling of 1400 Hz and thus an Al−H_B internuclear distance of 2.8 Å, where H_B is the Brønsted acid proton now bound to TMP. With this assumption, the maximum REDOR fraction that can be reached at long dephasing times is only 65%. There are significant differences between the experimental and calculated REDOR curves at longer dephasing times, and the assumption made in these calculations is clearly no longer valid at longer dephasing times. Furthermore, no oscillations are observed at long evolution times, as would be expected for a model consisting of an isolated spin pair.[20] Thus, the REDOR curves most likely contain at least two components associated with different dipolar couplings: one component with a large dipolar coupling governing REDOR responses during the first 1 ms, and the other component with a smaller dipolar coupling that becomes more apparent at longer evolution times. Importantly, it is not possible to fit the ^{27}Al/^{1}H REDOR curves with a *shorter* Al−H_B distance, and the curve fitting described above provides a measure of the *minimum* value for the Al−H_B distance for this complex. If the remaining ^{27}Al spins that were not presumed to be coupled to ^{1}H spins are included in the calculations and were assumed to be weakly coupled, this will result in a *longer* Al−H_B distance (see Figure 7b); this will be discussed in more detail below.

^{27}Al/^{1}H TRAPDOR NMR. Figure 8 shows the ^{27}Al/^{1}H TRAPDOR spectra for on-resonance ^{27}Al irradiation. Although the TRAPDOR fraction measured for the CH_3 protons is smaller than that for the P−H protons, it is not negligible (47% vs 31%). This indicates that some of the CH_3 spins are close to an aluminum atom. This is consistent with the dephasing observed in the ^{27}Al/^{1}H REDOR curves at longer dephasing times, where it was clear that there is an additional source of ^{27}Al/^{1}H REDOR dephasing other than that arising from coupling to the H_B proton.

Ab Initio Calculations: Structure of the Adsorption Complex. The most important parameters for the optimized structures of the hydrogen-bonded neutral complex (NC) and ion pair (IP) formed with TMP bound to the zeolite fragments Z_1H and Z_2H are given in Table 1, and the SCF/6-31G*-calculated structures of these complexes, with the Z_1H and Z_2H zeolite clusters, are shown in Figures 9 and 10, respectively. Inclusion of the correlation energy at the MP2 level resulted in a stronger interaction between $TMPH^+$/TMP and the zeolite cluster, by accounting for the dispersion effects between the adsorbed molecule and the zeolite cluster. This resulted in substantial decreases in the intermolecular H-bonds of the NC (H_B···P) and IP (O^-···H_B^+) structure of 0.25 and 0.3 Å on going from the SCF to the MP2 level calculations. The O−Al−O angle opens up for the IP structure, on increasing the cluster size from Z_1H to Z_2H, since two oxygen atoms act as binding sites in the Z_2H cluster, two symmetrically equivalent intermolecular O···H_B bonds being formed between the adsorbed $TMPH^+$ and these two oxygen atoms. A substantial decrease, from 4.1 Å in the NC to 3.3 Å in the IP, for the closest distance between a proton of a methyl group, H_M, and an aluminum atom in the Z_2

TABLE 1: Selected HF/6-31G*-Optimized Bond Lengths (Å) and Angles (deg) for the NC and IP Structures of Trimethylphosphine Bound to the Two Model Zeolite Clusters ($Z_1 = H_3SiOAlH_3$ and $Z_2 = H_3SiOAl-(O-SiH_3)_3$) Investigated[a]

	$Z_1H\cdots TMP$	$Z_1\cdots TMPH^+$	$Z_2H\cdots TMP$[b]	$Z_2\cdots TMPH^+$[b]
r(O−Si)	1.692 (1.709)	1.607 (1.645)	1.702	1.608
r(O−Al)	1.988 (1.982)	1.806 (1.856)	1.912	1.760
r(O−H_B)[c]	0.969 (1.013)	1.943 (1.646)	0.972	2.419
r(H_B−P)	2.408 (2.159)	1.386 (1.442)	2.375	1.374
r(Al−H_B)	2.530 (2.536)	2.703 (2.702)	2.491	2.869
r(Al−P)	4.080 (4.080)	3.680 (3.754)	4.355	3.691
r(Al−H_M)[d]	4.037 (3.706)	3.382 (3.703)	4.107	3.321
∠Si−O−Al	128.36 (126.00)	142.05 (136.01)	126.11	144.27
∠Al−O−H_B	113.09 (111.56)	103.01 (100.81)	115.54	85.17
∠P−H_B−O	168.76 (167.14)	166.00 (169.64)	170.83	121.77
∠P−H_B−Al	122.72 (120.53)	125.16 (127.20)	127.03	116.36

[a] The numbers in parentheses are those from structures calculated at the MP2/6-31G* level. [b] For the Z_2 model, O stands for the oxygen atom at the hydroxyl group. [c] H_B represents the proton associated with the Brønsted acid site. [d] H_M represents the proton at the methyl groups nearest to the aluminum atom.

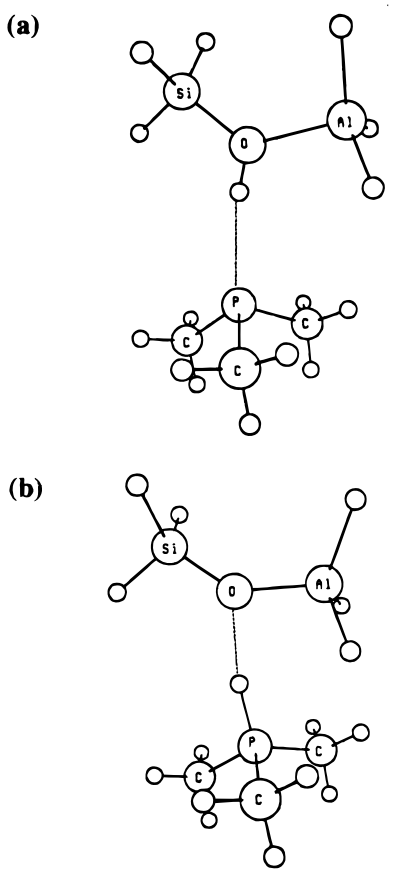

Figure 9. Schematic representation of the SCF/6-31G* calculated structures of the (a) TMP···Z_1H and (b) $TMPH^+\cdots Z_1^-$ complexes.

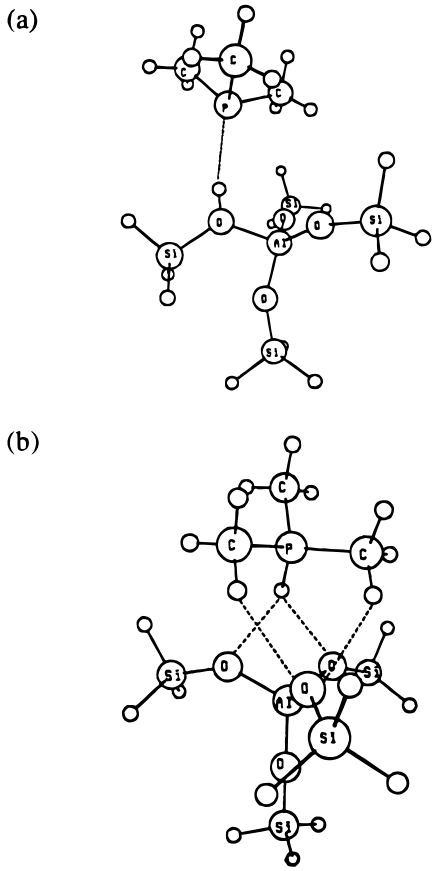

Figure 10. The SCF/6-31G* calculated structures of the (a) TMP···Z_2H and (b) $TMPH^+\cdots Z_2^-$ complexes.

cluster, is observed, indicating that the interaction between the oxygen atoms and methyl groups is significant in the IP structure. The Al−P and Al−H_B distances in the IP structure with the Z_2H zeolite model are 3.69 and 2.87 Å, respectively. The Al−P distance did not change significantly for the IP on going from the Z_1H to the Z_2H model, but an increase of 0.17 Å in the Al−H_B distance was observed. In contrast, the Al−P distance changed from 4.08 to 4.36 Å in the NC structure, on increasing the cluster size. In the NC structure, only one oxygen atom (associated with the Brønsted proton) acts as a binding site, for both zeolite models.

Ab Initio Calculations: Interaction and Proton-Transfer Energies. The proton-transfer energy (ΔE_{PT}) is defined as the difference between the energy of the IP complex and that of the NC complex (see Table 2). The IP complex was found to be less stable at the HF/6-31G* computational level. The IP structure becomes more stable on increasing the size of the zeolite fragment from the Z_1H to Z_2H model, the ΔE_{PT} values decreasing from 30.5 to 5.2 kJ mol^{-1} at the MP2 level. Thus, there appears to be a large dependence of the cluster size on the value of ΔE_{PT}. This suggests that larger clusters are needed to estimate the energetics of the complexes with higher reliability. The interaction energy (ΔE_{int}) was calculated as the difference between the total energy of the complex and the sum of energies of its subsystems. The interaction energy for the NC complex decreased by only 3.3 kJ mol^{-1} on going from the small zeolite cluster Z_1H to the larger zeolite cluster Z_2H, while it decreased by 9.0 kJ mol^{-1} for the IP complex at the MP2 level. Clearly, the size of the zeolite fragment has more influence on the IP structure because of the effect of charge separation. To assess how strongly our calculated interaction energies were affected by the BSSE, we carried out counterpoise

TABLE 2: Energetics of the Proton-Transfer Reaction for the NC and IP Complexes of TMP with the Z_1H Zeolite Model ($Z_1 = H_3SiOAlH_3$)[a]

	HF/6-31G*//HF/6-31G*	MP2/6-31G*//MP2/6-31G*
	Total Energy (au)	
TMP···Z_1H	−1069.3596552	1070.1884296
$TMPH^+$···Z_1^-	−1069.3497553	1070.1792557
Z_1^-	−609.2735109	−609.5961182
Z_1H	−609.7778464	−610.0960812
TMP	−459.5673738	−460.0681764
$TMPH^+$	−459.9449704	−460.4383223
	Relative Energy (kJ mol^{-1})	
ΔE_{PT}[b]	25.36 (2.64)	30.50 (5.19)
PA(zeolite)[c]	1288.56	1312.02
PA(TMP)	960.28	940.7
	ΔE_{int}(kJ mol^{-1})[d]	
TMP···Z_1H	−37.91 (−40.90)	59.66 (−62.90)
$TMPH^+$···Z_1^-	−344.74 (−329.89)	−375.27 (−366.31)
	BSSE (kJ mol^{-1})	
TMP···Z_1H	4.65 (6.18)	15.84 (14.91)
$TMPH^+$···Z_1^-	7.09 (15.27)	26.90 (35.62)
	ΔH_0 (kJ mol^{-1})[e]	
TMP···Z_1H	−28.11 (−30.54)	−39.05 (−43.79)
$TMPH^+$···Z_1^-	−331.27 (−308.18)	−345.09 (−324.25)

[a] Results for Z_2H ($Z_2 = H_3SiOAl-(O-SiH_3)_3$ are shown in parentheses. [b] $\Delta E_{PT} = E_{ion\ pair} - E_{neutral}$. [c] $PA = E(A) - E(AH) + ZPVE(A) - ZPVE(AH)$, where ZPVE is the zero-point vibrational energy. [d] $\Delta E_{int}(TMP\cdots Z_1H) = E(TMP\cdots Z_1H) - E(TMP) - E(Z_1H)$. $\Delta E_{int}(TMPH^+\cdots Z_1^-) = E(TMPH^+\cdots Z_1^-) - E(TMPH^+) - E(Z_1^-)$. [e] $\Delta H_o = \Delta E_{int} + \Delta ZPVE + BSSE$.

calculations. The BSSE was more significant for the IP complex (see Table 2). The interaction enthalpy at 0 K (ΔH_0) for the NC and IP complexes was also enhanced by increasing the size of the zeolite cluster. Unfortunately, the heat of adsorption of TMP in zeolites has not yet been reported, so no comparison with experiment could be made.

IV. Discussion

Comparison of the ab Initio and NMR Results. The experimental ^{31}P chemical shift and $^{31}P-^{1}H$ *J* couplings (of 550 Hz), at loading levels of less than or equal to 18 TMP/uc, show that an IP complex is formed, as was observed previously.[13,14] In contrast, our ab initio calculations were not able to determine unambiguously whether the IP or NC is the lower energy structure. We ascribe part of this discrepancy to the limited size of the zeolite fragment used in our calculations. Our calculations represent only the local bonding interactions and neglect the long-range electrostatic interactions which could have a considerable effect, given the partially ionic nature of the zeolite framework. Indeed, the IP complex becomes more stable with increased size of the zeolite clusters (from Z_1H to Z_2H). $TMPH^+$ was observed to interact with two oxygen atoms when the zeolite cluster Z_2H was used (Figure 10b). The greater surface curvature associated with a larger zeolite fragment also favors multiple coordination between the guest molecule and the lone pairs associated with oxygen atoms, increasing the stability of adsorption complexes. However, ab initio calculations involving large molecules interacting with larger zeolite models are computationally intensive if large basis sets are employed and geometry optimizations are performed. Brändle and Sauer[40,41] have explored one approach for overcoming this problem, where a cluster consisting of a sorbed molecule and a small zeolite fragment was embedded in a zeolite framework. The cluster was then described and optimized with full ab initio methods, while the periodic zeolite framework was optimized with semiempirical methods.[40,41] This allowed the influence of different zeolite frameworks to be explored.[40] In their study of NH_3 sorption on zeolite HY they found that the long-range potential contribution did enhance the stability of the IP complex relative to the NC complex, but that the difference was effectively canceled out by the limited relaxation of the zeolite framework cluster in the zeolite framework, resulting in little change between the value of ΔE_{PT} calculated for the cluster and that calculated for the cluster embedded in the periodic lattice.[41] Nonetheless, the long-range contribution of the potential to the reaction energies was considerable, and was 45% or −47.5 kJ mol^{-1} for NH_4^+ formation from the neutral gas species. The contribution decreased considerably as the cluster size was increased. Greatbanks et al. also embedded H-terminated clusters into a lattice of point charges, and they observed slightly larger values for the formation energy of NH_4^+ from the neutral species.[42] Unlike Brändle and Sauer they also observed large changes of 0.4−0.7 Å in the H−O distances on embedding the IP cluster in the point charges.

Comparing the distances obtained by REDOR NMR and ab initio calculations, the experimentally determined $^{31}P-^{27}Al$ distance is intermediate in value between the distances calculated for the NP and IC complexes. If the distances calculated using the larger cluster model are considered, our measured distance is much too short for the NC. However, the IP distances are calculated to be ∼0.2−0.25 Å shorter than the experimentally determined distances. A number of observations can be made: First, ab initio calculations may in some cases underestimate the distances. This is consistent with the high vibrational frequencies typically obtained by ab initio methods. Second, the ab initio values are those at 0 K; our experiments were performed at and above 123 K. Any vibrational motion and librations of the molecules on the surface will result in a longer measured distance. Finally, the effect of embedding the cluster in a periodic charged lattice with a restricted framework geometry has not been explored for this system. Given that the $^{27}Al/^{31}P$ REDOR measurement represents a maximum P−Al distance, it *is* consistent with the calculated distance of the IP complex.

We have performed simulations of the $^{31}P/^{27}Al$ TRAPDOR dephasing curves shown in Figure 6, to determine whether the TRAPDOR results are consistent with the distances obtained from the REDOR NMR and ab initio calculations. Experimental inputs of spinning speed (2.46 kHz) and the ^{27}Al rf field (58 kHz) as well as the asymmetry parameter η, internuclear distance, and relative orientations of the dipolar and quadrupolar tensors are needed, to calculate the TRAPDOR dephasing. A value for the QCC of 6.0 MHz, for ^{27}Al at the Brønsted acid site deprotonated by TMP, was obtained from TRAPDOR curves versus ^{27}Al offset frequency.[28] Since two angles are, however, required (for $\eta \neq 0$) to define the relative orientation of the dipolar and quadrupolar tensors, a large number of variables still remain to be determined, to extract accurate distances.

Recent ab initio calculations of the ^{27}Al QCC of the aluminum atoms in zeolite-like clusters, by van Santen and co-workers,[43] showed that the size and orientation of the electric field gradient tensor (EFG) is controlled by the nature of the four coordinated oxygen atoms of the AlO_4 tetrahedra. An AlO_4 with one protonated oxygen atom (O_1) has a large QCC of 11−18 MHz with $\eta < 0.5$. The principal axis of the EFG tensor, V_{zz}, is orientated along the $Al-O_1$ interatomic vector. In contrast, a deprotonated AlO_4, with two hydrogen-bonded oxygen atoms (O_1, O_2), which is formed by binding to methanol or ammonia,

has a moderate QCC of 5−10 MHz with $\eta > 0.5$. V_{zz} now is orientated perpendicular to the O_1-Al-O_2 plane. This latter model is similar to the local environment for $TMPH^+$ coordinated to the Z_2H cluster, determined from our ab initio calculations, suggesting that a similar orientation of the EFG tensor may be present in this system. A reasonably good fit to the TRAPDOR curve was achieved with a P−Al distance of 3.8 Å, $\eta = 0.7$, and an angle between the Al−P internuclear vector and V_{zz} of 90° (V_{yy} was oriented along the Al−P vector) (Figure 6). This distance is very close to that obtained from the ab initio calculations for the IP cluster (Table 1). We note that while this distance is consistent with our calculated distance and close to the measured distance (by REDOR NMR), the TRAPDOR method used here cannot be used as an independent technique for extracting distances: When relative orientations of the dipolar and quadrupolar tensors and values for η were chosen so as to produce the maximum (V_{zz} is collinear with the Al−P internuclear vector and $\eta = 0$) and minimum (V_{yy} is collinear with the Al−P vector and $\eta = 0$) TRAPDOR dephasings, values for the internuclear distances of 3.4 and 4.4. Å, respectively, were required to simulate the TRAPDOR dephasing curves. The TRAPDOR simulations are also sensitive to the exact value of the offset used in the simulations, which introduces further sources of error. This is discussed in more detail in ref 44. We are currently testing the REAPDOR experiment,[45] a variant of the TRAPDOR method which is less sensitive to the relative orientation of the dipolar and quadrupolar tensors,[45,46] to determine whether more reliable distances may be obtained. Alternatively it may be possible to perform a separated local field type experiment to determine the relative orientation of the dipolar and quadrupolar tensors (see, e.g., ref 47). This should help to improve the accuracy and reliability of the TRAPDOR curve fitting, for distance measurement in cases where the REDOR method cannot be reliably applied.

Spin Counting and Al−H Distance Measurements. The measured values of 0.6:1 to 0.8:1 for the ^{31}P: visible ^{27}Al ratio indicate that some of the aluminum T-sites that are not directly bound to TMP are visible when using MAS methods. This was not observed for our previous MMA studies where a 1:1 correspondence between loading level and visible ^{27}Al spins was found. One explanation for this is that the presence of other sorbed species such as H_2O and residual ammonia ions, which were not removed during the dehydration process, may result in reduced QCCs. The ^1H MAS NMR of the bare material was not, however, consistent with this suggestion. Another possibility is that the relatively large TMP molecule, in comparison to MMA, may interact with other T-groups on the zeolite framework. In particular, the hydrogen atoms of the CH_3 groups may be weakly bound to the framework, reducing the QCC slightly of some of the framework sites, making some of the Brønsted acid sites visible. Both the $^{27}Al/^1H$ REDOR and TRAPDOR data are consistent with this suggestion (vide infra). Finally, LZY-62 is known to contain some sodium cations. In a different sample of LZY-62 obtained from Aldrich Chemical, ICP analysis indicated that the Na^+ content was as much as 10 Na/unit cell. The QCC of aluminum atoms in dehydrated NaY is significantly smaller than that in HY.[48] Sites associated with Na^+ cations will therefore have reduced QCCs, and these sites may be visible.

The fit to the Al−H REDOR data, based on the isolated Al−H spin pair model, was not satisfactory at long evolution times. At least some of these visible aluminum spins must be weakly bound to protons, since the maximum value in the $^{27}Al/^1H$ REDOR dephasing curve after 2 ms of dephasing (80%) is larger than predicted for coupling to the Brønsted acid−TMP proton only (65%). This statement is also consistent with the $^{27}Al/^1H$ TRAPDOR data, where a TRAPDOR effect was also observed for the methyl groups, indicating that they are close to the aluminum atoms. We have performed a whole series of simulations, to examine the effect of other coupled protons (other than from the P−H group) on the $^{27}Al-^1H_B$ distance as measured by REDOR NMR. In all these simulations, we required a longer $Al-H_B$ distance, to fit the experimental data. One representative example is shown in Figure 7b, where we have assumed that 15% of the visible aluminum spins are due to non-TMP-complexed Brønsted acid sites that are actually visible, possibly due to a weak interaction with the methyl groups of TMP, and contribute to the dephasing. A typical $^{27}Al-^1H_B$ distance of 2.45 Å[49,50] (corresponding to an $^{27}Al/^1H$ dipolar coupling constant of 2120 Hz) was assumed, and the number of visible Brønsted acid sites was chosen on the basis of the difference between the expected REDOR fraction (65%) for the 1:1 complex and the experimentally observed value at longer dephasing times (80%). To obtain the best fit to the curve with this model, a smaller Al−H dipolar coupling constant of 1 kHz was required. This corresponds to a distance of 3.10 Å. All other simulations performed by assuming that a larger percentage of the aluminum atoms (i.e., >15%) are due to Brønsted acid sites not directly coordinated to TMP resulted in REDOR fractions at longer dephasing times that are greater than those observed experimentally. Thus, the $Al-H_B$ distance extracted assuming an isolated pair model (2.8 Å) must represent the minimum distance, and it is likely that the real $Al-H_B$ distance is slightly longer, but no longer than 3.1 Å. Note that the ab initio distances are 2.7−2.9 Å for the IP complex; the calculated values for the NC are significantly shorter.

Ab initio results show that the $^{27}Al-^1H$ distance between the aluminum atom and the protons of the methyl groups (H_M) nearest to the aluminum atom may be as short as 3.3 Å (see Table 2). This $Al-H_M$ distance corresponds to an $^{27}Al-^1H$ dipolar coupling constant of 826 Hz. Rapid motion of CH_3 groups will, however, scale the dipolar coupling, and the additional Al−H dephasing due to this dipolar coupling will not be as large as this dipolar coupling constant suggests. Unfortunately, a full analysis of the methyl groups' contribution to the $^{27}Al/^1H$ REDOR dephasing curve is complicated, and we have not, as yet, attempted it. Fripiat et al.[10,51] have reported that a combination of one-pulse and CP REDOR NMR experiments allows one to distinguish the contributions from nuclei with different heteronuclear second moments. We note, however, that this method requires large differences between the second moments of the different species, which is not necessarily the case here. The use of the deuterated TMP may be one possible solution to this problem, and we are currently in the process of repeating these measurements with deuterated TMP, to reduce the "background" signal from the additional Al−H couplings.

Figure 11 compares the calculated and all the measured distances. The $Al-H_B-P$ angle was determined by using a distance of 1.4 Å for the $P-H_B$ bonds. This was previously determined by Lunsford et al., and was also extracted from our simulations of the ^1H spectra. Depending on the $Al-H_B$ distance used, the $Al-H_B-P$ angle varies between 118° and 138°. Despite the errors associated with the $Al-H_B$ distance NMR measurement, both the NMR and ab initio calculations show that the TMP molecule tilts toward the surface, presumably to allow additional van der Waals interactions between the methyl groups and the oxygen framework sites.

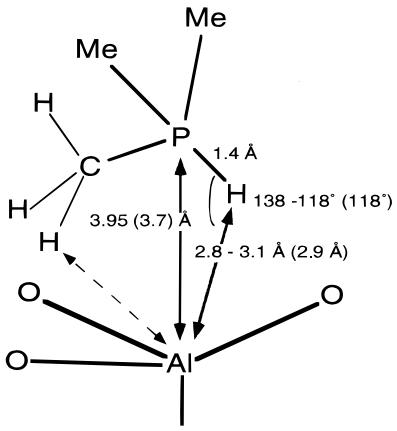

Figure 11. A comparison of the experimental and calculated distances. Calculated distances and angles obtained for the $TMPH^{+}-Z_2^{-}$ cluster are given in parentheses. The dashed line indicates that an interaction between the two spins was observed experimentally, but the distance was not quantified.

V. Conclusions

A combination of experiments and calculations were required to probe the binding of TMP to zeolite HY: ab initio calculations alone were unable to determine whether the NC or IP structure is the lower energy structure. Calculations indicated that the NC structure was more stable than the IP structure, contrary to the ^{31}P MAS NMR observations. However, the IP structure became more stable as the cluster size was increased. NMR distance measurements involving relatively isolated spin pairs such as $^{31}P-^{27}Al$ allowed accurate distance information to be obtained at low temperatures. An A1−P distance of 3.95 (+0.05) Å was determined for the rigid complex bound to the zeolite framework from $^{27}Al/^{31}P$ REDOR NMR curves measured as a function of temperature. Since no change in the measured distance was observed between −50 and −150 °C, the error due to any residual motion or small librational motions is not believed to be significant. It is not possible at this moment to totally exclude the possibility that small librational motions may result in a measured distance that is slightly longer than the actual distance. Given that no change in the measured distance is observed between −50 and −150 °C, the error is not, however, believed to be significant. As a further check of motion, we have measured a known distance, namely, the P−H distance. This measurement is in line with known P−H distances for trimethylphosphines, and acts as a control, excluding the possibility of any significant librations that involve the P−H groups. 2D ^2H NMR experiments,[52] which can probe motion that occurs on the REDOR time scale, are planned to determine whether these experiments can act as an even more sensitive method for excluding the possibility of motion. An estimate of the $Al-H_B$ distance of 2.8−3.1 Å was obtained from $^{27}Al/^{1}H$ REDOR NMR experiments for this complex; more accurate distance measurements were not possible, since the assumption of an isolated Al−H spin pair model is not valid in this case.

Improved structure prediction will result if (a) more internuclear distances are measured and (b) systems with isolated spin pairs (or well-defined spin clusters) are studied. As more and more distances are measured, distance constraints become tighter, even if the accuracy of the NMR experiment does not improve. Measurement of some known distances or "controls" should help exclude the possibility of inaccurate distance measurements resulting from residual molecular motion. Finally, the $^{27}Al/^{31}P$ REDOR NMR experiment is relatively straightforward and can be easily applied to study binding of phosphorus-containing molecules to aluminum surfaces. Analogous experiments containing other bound molecules and spin pairs such as $^{27}Al/^{19}F$ and $^{27}Al/^{77}Se$ may readily be envisaged.

Acknowledgment is made to the donors of the Petroleum Research Fund, administered by the American Chemical Society, and the National Science Foundation National Young Investigator program (Grant DMR-9458017) for support of this research. The solid-state NMR spectrometer was purchased with a grant from the National Science Foundation (CHE-9405436). J.C.J. and S.H.L. thank the National Science Counsel of Taiwan for financial support.

References and Notes

(1) Corma, A. *Chem. Rev.* **1995**, *95*, 559.
(2) Farneth, W. E.; Gorte, R. J. *Chem. Rev.* **1995**, *95*, 615.
(3) van Santen, R. A.; Kramer, G. J. *Chem. Rev.* **1995**, *95*, 637.
(4) (a) Sauer, J.; Ugliengo, P.; Garrone, E.; Saunders: V. R. *Chem. Rev.* **1994**, *94*, 2095. (b) Haw, J. F.; Nicholas, J. B.; Xu, T.; Beck, L. W.; Ferguson, D. B. *Acc. Chem. Res.* **1996**, *29*, 259.
(5) (a) Pelmenschikov, A. G.; van Santen, R. A.; Jänchen, J.; Meijer, E. *J. Phys. Chem.* **1993**, *97*, 11071. (b) Haw, F. J.; Hall, M. B.; Alvarado-Swaisgood, A. E.; Munson, E. J.; Lin, Z.; Beck, L. W.; Howard, T. *J. Am. Chem. Soc.* **1994**, *116*, 7308. (c) Sepa, J.; Gorte, R. J.; White D.; Kassab, E.; Allavena, M. *Chem. Phys. Lett.* **1996**, *262*, 321.
(6) (a) Mirth, G.; Lercher, J. A.; Anderson, M. W.; Klinowski, J. *J. Chem. Soc., Faraday Trans.* **1990**, *86*, 3039. (b) Kubelkobá, L.; Nováková, J. *Zeolites* **1991**, *11*, 882. (c) Florián, J.; Kubelkobá, L. *J. Phys. Chem.* **1994**, *98*, 8734. (d) Zicovich-Wilson, C. M.; Viruela, P.; Corma, A. *J. Phys. Chem.* **1995**, *99*, 13224.
(7) (a) Luz, Z.; Vega, A. J. *J. Phys. Chem.* **1987**, *91*, 374. (b) Mirth, G.; Lercher, J. A.; Anderson, M. W.; Klinowski, J. *J. Chem. Soc., Faraday Trans.* **1990**, *86*, 3039. (c) Haase, F.; Sauer, J. *J. Am. Chem. Soc.* **1995**, *117*, 3780. (d) Haase, F.; Sauer, J. *J. Phys. Chem.* **1994**, *98*, 8, 3083. (e) Shah, R.; Payne, M. C.; Lee, M.-H.; Gale, J. D. *Science* **1996**, *271*, 1395.
(8) (a) Marchese, L.; Wright, P. A.; Thomas, J. M. *J. Phys. Chem.* **1993**, *97*, 8109. (b) Smith, L.; Cheetham, A. K.; Morris, R. E.; Marchese, L.; Thomas, J. M.; Wright, P. A.; Chen, J. *Science* **1996**, *271*: 799.
(9) Grey, C. P.; Kumar, B. S. A. *J. Am. Chem. Soc.* **1995**, *117*, 9071.
(10) (a) Coster, D.; Blumenfeld, A.; Fripiat, J. J. *J. Phys. Chem.* **1994**, *98*, 6201. (b) Blumenfeld, A. L.; Fripiat, J. J. *J. Phys. Chem. B* **1997**, *101*, 6670.
(11) Kao, H. M.; Grey, C. P. *J. Am. Chem. Soc.* **1997**, *119*, 627−628.
(12) (a) Teunissen, E. H.; van Duijnevedlt, F. B.; van Santen, R. A. *J. Phys. Chem.* **1992**, *96*, 366. (b) Teunissen, E. J.; van Santen, R. A.; Jansen, A. P.; van Duijneveldt, F. B. *J. Phys. Chem.* **1993**, *97*, 203.
(13) Rothwell, W. P.; Shen, W.; Lunsford, J. H. *J. Am. Chem. Soc.* **1984**, *106*, 2452.
(14) Chu, P. J.; Carvajal, R. R.; Lunsford, J. H. *Chem. Phys. Lett.* **1990**, *175*, 407.
(15) Bendada, A.; DeRose, E.; Fripiat, J. J. *J. Phys. Chem.* **1994**, *98*, 3838.
(16) Riemer, T.; Knözinger, H. *J. Phys. Chem.* **1996**, *100*, 6739.
(17) Lunsford, J. H. *Top. Catal.* **1997**, *4*, 91.
(18) Zhao, B.; Pan, H.; Lunsford, J. H. *Langmuir* **1999**, *15*, 2761.
(19) Kao, H. M.; Grey, C. P. *Chem. Phys. Lett.* **1996**, *259*, 459.
(20) Kao, H. M.; Grey, C. P.; Pitchumani, K.; Lakshminarasimhan, P. H.; Ramamurthy, V. *J. Phys. Chem.* **1998**, *102*, 5627.
(21) (a) Fyfe, C. A.; Diaz, A. C.; Lewis, A. R.; Chezeau, J. M.; Grondey, H.; Kokotailo, G. T. *ACS Symp. Ser.* **1999**, *717*, 283. (b) Lewis, A. Ph.D. Thesis, The University of British Columbia, 1998.
(22) (a) Gullion, T.; Schaefer, J. *J. Magn. Reson.* **1989**, *81*, 196. (b) Gullion, T.; Schaefer, J. In *Advances in Magnetic Resonance*; Warren, W. S., Ed.; Academic Press: New York, 1989; Vol. 13, p 57.
(23) Garbow, J. R.; Gullion, T. *J. Magn. Reson.* **1991**, *95*, 442.
(24) Grey, C. P.; Vega, A. *J. Am. Chem. Soc.* **1995**, *117*, 8232.
(25) Ernst, H.; Freude, D.; Wolf, I. *Chem. Phys. Lett.* **1993**, *212*, 558.
(26) Kao, H. M.; Grey, C. P. *J. Phys. Chem.* **1996**, *100*, 5105.
(27) Rakiewicz, E. F.; Peters, A. W.; Wormsbecher, R. F.; Sutovich K. J.; Mueller, K. T. *J. Phys. Chem. B* **1998**, *102*, 2890.
(28) Kao, H. M. Ph.D. Thesis, State University of New York at Stony Brook, 1998.
(29) Luz, Z.; Vega, A. J. *J. Phys. Chem.* **1987**, *91*, 365.
(30) Fenzke, D.; Freude, D.; Frohlich, T.; Haase, J. *Chem. Phys. Lett.* **1984**, *111*, 171.
(31) Massiot, D.; Bessada, C.; Coutures, J. P.; Taulelle, F. *J. Magn. Reson.* **1990**, *90*, 231.
(32) Naito, A.; Nishimura, K.; Kimura, S.; Tuzi, S.; Aida, M.; Yasuoka, N.; Saito, H. *J. Phys. Chem.* **1996**, *100*, 14995.

(33) Vega, A., Grey, C. P. Unpublished results.
(34) Frisch, M. J.; Trucks, G. W.; Head-Gordon, M.; Gill, P. M. W.; Wong, M. W.; Foresman, J. B.; Johnson, B. G.; Schlegel, H. B.; Robb, M. A.; Replogle, E. S.; Gomperts, R.; Andres, J. L.; Raghavachari, K.; Binkley, J. S.; Gonzalez, C.; Martin, R. L.; Fox, D. J.; Defrees, D. J.; Baker, J.; Stewart, J. J. P.; Pople, J. A. *GAUSSIAN 92*; Gaussian, Inc.: Pittsburgh, PA, 1992.
(35) Roothaan, C. C. J. *Rev. Mod. Phys.* **1951**, *23*, 69.
(36) Møller, C.; Plesset, M. S. *Phys. Rev.* **1934**, *46*, 618.
(37) Boys, S. F.; Bernardi, F. *Mol. Phys.* **1970**, *19*, 553.
(38) Jacobs, W. P. J. H.; de Haan, J. W.; van de Ven, L. J. M.; van Santen, R. A. *J. Phys. Chem.* **1993**, *97*, 10394.
(39) (a) Bartelli, L. S.; Hirst, R. C. *J. Chem. Phys.* **1959**, *31*, 449. (b) Durig, J. R.; Carreira L. A.; Odom, J. D. *J. Am. Chem. Soc.* **1974**, *96*, 2688.
(40) Brändle, M.; Sauer, J. *J. Am. Chem. Soc.* **1998**, *120*, 1556.
(41) Brändle, M.; Sauer, J. *J. Mol. Catal. A* **1997**, *119*, 19.
(42) Greatbanks, S. P.; Sherwood, P.; Hillier, I. H.; Hall, R. J.; Burton, N. A.; Gould, I. R. *Chem. Phys. Lett.* **1997**, *234*, 367.
(43) Koller, H.; Meijer, E. L., van Santen, R. A. *Solid State Nucl. Magn. Reson.* **1997**, *9*, 165.
(44) Liu, H.; Grey, C. P. Manuscript in preparation.
(45) (a) Gullion, T. *Chem. Phys. Lett.* **1995**, *246*, 325. (b) Gullion, T. *J. Magn. Reson. A* **1995**, *117*, 326.
(46) Ba, Y.; Kao, H. M.; Grey, C. P.; Chopin, L.; Gullion, T. *J. Magn. Reson.* **1998**, *133*, 104.
(47) van Eck, E. R. H.; Smith, M. E. *J. Chem. Phys.* **1998**, *108*, 5904.
(48) Freude, D.; Haase, J. *Nucl. Magn. Reson. Basic Principles Prog.* **1993**, *29*, 1.
(49) Freude, D.; Klinowski, J.; Hamdan, H. *Chem. Phys. Lett.* **1988**, *149*, 355.
(50) Hunger, M.; Freude, D.; Fenzke, D.; Pfeifer, H. *Chem. Phys. Lett.* **1992**, *191*, 391.
(51) Blumenfeld, A. L.; Coster, D.; Fripiat, J. J. *Chem. Phys. Lett.* **1994**, *231*, 497.
(52) Schmidt, C.; Wefing, S.; Blümich, B.; Spiess, H. W. *Chem. Phys. Lett.* **1986**, *130*, 84.